



(11) **EP 2 805 784 A1**

(12) **EUROPEAN PATENT APPLICATION**

(43) Date of publication:  
**26.11.2014 Bulletin 2014/48**

(51) Int Cl.:  
**B22F 5/04 (2006.01) C22C 19/05 (2006.01)**

(21) Application number: **14157622.3**

(22) Date of filing: **04.03.2014**

(84) Designated Contracting States:  
**AL AT BE BG CH CY CZ DE DK EE ES FI FR GB  
GR HR HU IE IS IT LI LT LU LV MC MK MT NL NO  
PL PT RO RS SE SI SK SM TR**  
Designated Extension States:  
**BA ME**

(30) Priority: **24.05.2013 GB 201309404**  
**22.10.2013 GB 201318622**

(71) Applicant: **Rolls-Royce plc**  
**London SW1E 6AT (GB)**

(72) Inventors:  
• **Hardy, Mark**  
**Belper, Derbyshire DE56 2UP (GB)**

- **Stone, Howard**  
**Cambridge, CB24 9IT (GB)**
- **Mignanelli, Paul**  
**Cambridge, GB CB3 9BB (GB)**
- **Conduit, Bryce**  
**Fareham, GU9 9JU (GB)**
- **Conduit, Gareth**  
**Cambridge, CB2 1TA (GB)**

(74) Representative: **Gee, Philip David et al**  
**Rolls-Royce plc**  
**Intellectual Property**  
**SinB-38, PO Box 31**  
**Derby**  
**Derbyshire DE24 8BJ (GB)**

(54) **A nickel alloy**

(57) A nickel- base alloy having the following composition (in weight percent unless otherwise stated): Cr 10.5-15.0; Co 1.7-8.8; Fe 0-5.9; Si 0-0.65; Mn 0-0.65; Mo 0.3-2.3; W 2.3-4.4; Al 2.7-4.1; Nb 1.0-4.2; Ti 1.0-3.0; Ta 2.0-5.0; Hf 0.0-0.6; C 0.02-0.06; B 0.015-0.035; Zr 0.035-0.11; S < 20ppm; P < 60ppm; the balance being

Ni and incidental impurities. The alloy has an improved combination of properties (principally resistance to surface environmental damage and dwell fatigue crack growth) compared with known alloys, and is intended to operate for prolonged periods of time above 700 °C, and up to peak temperatures of 800°C.

**EP 2 805 784 A1**

**Description**

**[0001]** This invention relates to nickel (Ni) base alloys, and particularly, though not exclusively, to alloys suitable for use in compressor and turbine discs of gas turbine engines. Such discs are critical components of gas turbine engines, and failure of such a component in operation can be catastrophic.

**[0002]** There is a continuing need for improved alloys to enable disc rotors in gas turbine engines, such as those in the high pressure (HP) compressor and turbine, to operate at higher compressor outlet temperatures and faster shaft speeds. These facilitate the high climb ratings that are increasingly required by commercial airlines to move aircraft more quickly to altitude, to reduce fuel burn and to get the aircraft away from the busy air spaces around airports. These operating conditions give rise to fatigue cycles with long dwell periods at elevated temperatures, in which oxidation and time dependent deformation significantly influence the resistance to low cycle fatigue. As a result, there is a need to improve the resistance of alloys to surface environmental damage and dwell fatigue crack growth, and to increase proof strength, without compromising their other mechanical and physical properties or increasing their density.

**[0003]** Known alloys cannot provide the balance of properties needed for such operating conditions, in particular damage tolerance performance under dwell cycles at temperatures in the range of 600°C to 800°C, resistance to environmental damage, microstructural stability and high levels of proof strength. As such, they are not good candidates for disc applications at peak temperatures of 750°C to 800°C, because component lives would be unacceptably low.

**[0004]** Some known nickel base alloys have compromised resistance to surface environmental degradation (oxidation and Type II hot corrosion) in order to achieve improved high temperature strength and resistance to creep strain accumulation, and in order to achieve stable bulk material microstructures (to prevent the precipitation of detrimental topologically close-packed phases). Turbine discs are commonly exposed to temperatures above 650°C, and in future engine designs will be exposed to temperatures above 700°C. As disc temperatures continue to increase, oxidation and hot corrosion damage will begin to limit disc life. There is therefore a need, in the design of future disc alloys, to prioritise resistance to dwell crack growth and oxidation and hot corrosion damage ahead of other properties.

**[0005]** Without suitable alloys, environmental protection will need to be applied to discs, which is undesirable and technically very difficult.

**[0006]** It is an aim of the invention to provide a nickel base alloy that can operate for prolonged periods of time above 700°C, and up to peak temperatures of 800°C.

**[0007]** The invention provides a nickel base alloy, and a method of making such an alloy, as set out in the claims.

**[0008]** The invention will be more fully described, by way of example only, with reference to the accompanying drawings in which:

Figure 1 shows predicted phases in alloy V207S125C as a function of temperature;

Figure 2 shows predicted phases in alloy V207S135A as a function of temperature;

Figure 3 shows predicted elemental content of gamma ( $\gamma$ ) phase in alloy V207S135B as a function of temperature;

Figure 4 shows the predicted partitioning of silicon (Si) in the  $\gamma$  and  $\gamma'$  phases as a function of temperature for alloy V207S125E;

Figure 5 shows the predicted partitioning of manganese (Mn) in the  $\gamma$  and  $\gamma'$  phases as a function of temperature for alloy V207S125A; and

Figure 6 shows the predicted elemental content of MC carbide in alloy V207S125A as a function of temperature.

**[0009]** In defining the compositions of alloys according to the invention, the aim was to produce alloys in which the disordered face-centred cubic gamma ( $\gamma$ ) phase is precipitation strengthened by the ordered  $L1_2$  gamma prime ( $\gamma'$ ) phase.

**[0010]** The inventors have determined that the following two groups of compositions produce the required balance between high temperature proof strength, resistance to fatigue damage and creep strain accumulation, damage tolerance and oxidation / hot corrosion damage. Within these two groups, the first group (examples of which are shown in Table 1) has a bias towards providing a higher resistance to oxidation / hot corrosion damage and shows a minimum amount of strengthening precipitates that is necessary to provide the required high temperature proof strength and resistance to creep strain accumulation. This resistance to environmental damage is superior to that shown by existing powder nickel alloys that are currently used for disc rotor applications. Whereas, the second group (examples of which are shown in Table 2) shows a level of environmental resistance, which is at least equivalent or better than the existing powder nickel alloys but offers a higher level of high temperature proof strength and resistance to creep strain accumulation than the first group of compositions.

**[0011]** To achieve the required proof strength and resistance to creep strain accumulation, at least 48 mole % of fine  $\gamma'$  ( $\text{Ni}_3\text{X}$ ) particles should be precipitated at 800°C, where X is aluminium (Al), titanium (Ti), niobium (Nb), tantalum (Ta), or silicon (Si). Combinations of these elements are added such that in atomic %,

$$\text{Al} + \text{Ti} + \text{Nb} + \text{Ta} + 0.3\text{Si} = 12.5 \text{ at.}\% \quad (\text{Group 1})$$

$$\text{Al} + \text{Ti} + \text{Nb} + \text{Ta} + 0.3\text{Si} = 13.5 \text{ at.}\% \quad (\text{Group 2})$$

in which Al can have values from about 6.5 to about 8.25 at.%, Ti can have values between about 2.25 and about 3.5 at.%, Nb can have values between about 0.75 and about 2.25 at.%, Ta can have values between about 0.75 and about 1.5 at.% and Si can have values between zero and about 1.2 at%. Phase diagram modelling, using JMat Pro version 6.1 and the Thermotech Nickel-8 database, indicates that Group 1 and 2 alloys are expected to have 48-50 and 53-55 mole % of  $\gamma'$  precipitates respectively at 800°C. The predicted content of  $\gamma'$  and other phases are shown in Figures 1 and 2 for alloys V207S125C and V207S135A respectively at temperatures between the respective liquidus temperatures and 600°C. Table 3 also provides the predicted mole % of  $\gamma'$  at 800°C for the proposed compositions and other solvus data, which will be discussed later.

Table 1 - Group 1 example compositions in atomic (at. %) and weight (wt. %) percent

at. %	Ni	Cr	Co	Fe	Mo	W	Mn	Al	Ti	Ta	Nb	Hf	Si	C	B	Zr
V207S125A	Bal.	15.00	3.0	4.5	0.35	0.9	0.60	7.00	2.50	1.00	2.00	0.0	0.00	0.150	0.160	0.0375
V207S125B	Bal.	15.50	3.0	4.5	0.35	0.9	0.60	7.00	2.50	1.00	2.00	0.0	0.00	0.150	0.160	0.0375
V207S125C	Bal.	15.00	3.0	4.5	0.35	0.9	0.60	7.00	3.00	1.00	1.50	0.0	0.00	0.150	0.160	0.0375
V207S125D	Bal.	15.00	3.0	4.5	0.35	0.9	0.60	7.00	3.00	1.00	1.50	0.1	0.00	0.150	0.160	0.0375
V207S125E	Bal.	14.00	3.0	4.5	0.35	0.9	0.60	7.00	2.50	1.00	1.70	0.0	1.15	0.150	0.160	0.0375
V207S125F	Bal.	15.00	3.0	4.5	0.35	0.9	0.00	7.00	2.50	1.00	2.00	0.0	0.00	0.150	0.160	0.0375
V207S125G	Bal.	14.75	3.0	4.5	0.35	1.1	0.60	7.25	2.50	1.00	1.75	0.0	0.00	0.150	0.160	0.0375
V207S125H	Bal.	14.75	3.0	4.5	0.35	1.1	0.60	7.50	2.50	1.25	1.25	0.0	0.00	0.150	0.160	0.0375
V207S125I	Bal.	14.75	2.0	5.5	0.35	1.0	0.60	7.25	2.50	1.25	1.50	0.0	0.00	0.150	0.160	0.0375
V207S125J	Bal.	15.25	4.0	3.5	0.35	1.1	0.60	7.25	2.50	1.25	1.50	0.0	0.00	0.150	0.160	0.0375
V207S125K	Bal.	15.25	4.0	3.5	0.35	1.0	0.60	7.25	2.50	1.50	1.25	0.0	0.00	0.145	0.135	0.0350
V207S125L	Bal.	15.25	4.0	3.5	0.35	1.0	0.58	7.75	2.50	1.50	0.75	0.0	0.00	0.242	0.135	0.0350
V207S125M	Bal.	14.75	4.0	0	1.15	1.2	0.59	7.35	2.75	1.50	0.90	0.0	0.00	0.245	0.135	0.0355
wt. %	Ni	Cr	Co	Fe	Mo	W	Mn	Al	Ti	Ta	Nb	Hf	Si	C	B	Zr
V207S125A	Bal.	13.40	3.0	4.3	0.60	2.8	0.57	3.30	2.10	3.10	3.20	0.0	0.00	0.030	0.030	0.060
V207S125B	Bal.	13.90	3.0	4.3	0.60	2.9	0.57	3.30	2.10	3.10	3.20	0.0	0.00	0.030	0.030	0.060
V207S125C	Bal.	13.50	3.1	4.3	0.60	2.9	0.57	3.30	2.50	3.10	2.40	0.0	0.00	0.030	0.030	0.060
V207S125D	Bal.	13.50	3.0	4.3	0.60	2.9	0.57	3.30	2.50	3.10	2.40	0.3	0.00	0.030	0.030	0.060
V207S125E	Bal.	12.60	3.1	4.4	0.60	2.9	0.57	3.30	2.10	3.10	2.70	0.0	0.56	0.030	0.030	0.060
V207S125F	Bal.	13.50	3.1	4.4	0.60	2.9	0.00	3.30	2.10	3.10	3.20	0.0	0.00	0.030	0.030	0.060
V207S125G	Bal.	13.20	3.0	4.3	0.60	3.5	0.57	3.40	2.10	3.10	2.80	0.0	0.00	0.030	0.030	0.060
V207S125H	Bal.	13.20	3.0	4.3	0.60	3.5	0.57	3.50	2.10	3.90	2.00	0.0	0.00	0.030	0.030	0.060
V207S125I	Bal.	13.20	2.0	5.3	0.60	3.2	0.57	3.40	2.10	3.90	2.40	0.0	0.00	0.030	0.030	0.060
V207S125J	Bal.	13.60	4.0	3.3	0.60	3.5	0.56	3.30	2.00	3.90	2.40	0.0	0.00	0.030	0.030	0.060
V207S125K	Bal.	13.60	4.0	3.3	0.60	3.1	0.56	3.30	2.00	4.60	2.00	0.0	0.00	0.030	0.025	0.055

5  
  
10  
  
15  
  
20  
  
25  
  
30  
  
35  
  
40  
  
45  
  
50  
  
55

(continued)

wt. %	Ni	Cr	Co	Fe	Mo	W	Mn	Al	Ti	Ta	Nb	Hf	Si	C	B	Zr
V207S125L	Bal.	13.60	4.1	3.4	0.60	3.2	0.55	3.60	2.10	4.70	1.20	0.0	0.00	0.050	0.025	0.055
V207S125M	Bal.	13.00	4	0	1.90	3.6	0.55	3.40	2.25	4.60	1.40	0.0	0.00	0.050	0.025	0.055

Table 2 - Group 2 example compositions in atomic (at. %) and weight (wt. %) percent

at. %	Ni	Cr	Co	Fe	Mo	W	Mn	Al	Ti	Ta	Nb	Hf	Si	C	B	Zr
V207S135A	Bal.	13.50	3.0	4.5	0.35	0.9	0.60	7.25	3.00	1.25	2.00	0.0	0.00	0.150	0.160	0.0375
V207S135B	Bal.	12.50	3.0	4.5	0.35	0.9	0.60	7.00	3.25	1.00	1.95	0.0	1.15	0.150	0.160	0.0375
V207S135C	Bal.	13.50	3.0	4.5	0.35	0.9	0.00	7.25	3.00	1.25	2.00	0.0	0.00	0.150	0.160	0.0375
V207S135D	Bal.	12.75	3.0	4.5	0.35	1.1	0.60	7.25	3.00	1.25	2.00	0.0	0.00	0.150	0.160	0.0375
V207S135E	Bal.	13.25	3.0	4.5	0.35	1.0	0.60	7.75	3.00	1.50	1.25	0.0	0.00	0.150	0.160	0.0375
V207S135F	Bal.	12.75	2.0	5.5	0.35	0.9	0.60	7.50	3.00	1.25	1.75	0.0	0.00	0.150	0.160	0.0375
V207S135G	Bal.	13.25	4.0	3.5	0.35	1.1	0.60	7.50	3.00	1.25	1.75	0.0	0.00	0.150	0.160	0.0375
V207S135H	Bal.	13.75	4.0	3.5	0.35	1.0	0.60	7.75	3.00	1.50	1.25	0.0	0.00	0.145	0.135	0.0350
V207S135I	Bal.	13.75	4.0	3.5	0.35	1.0	0.59	7.75	3.00	1.50	1.25	0.1	0.00	0.145	0.135	0.0350
V207S135J	Bal.	13.75	4.0	3.5	0.35	1.0	0.59	7.75	3.25	1.50	1.00	0.0	0.00	0.245	0.135	0.0350
V207S135K	Bal.	13.50	4.0	3.5	0.90	1.0	0.59	7.50	3.50	1.50	1.00	0.0	0.00	0.245	0.135	0.0350
wt. %	Ni	Cr	Co	Fe	Mo	W	Mn	Al	Ti	Ta	Nb	Hf	Si	C	B	Zr
V207S135A	Bal.	12.00	3.0	4.3	0.60	2.8	0.56	3.40	2.50	3.90	3.20	0.0	0.00	0.030	0.030	0.060
V207S135B	Bal.	11.20	3.1	4.3	0.60	2.9	0.57	3.30	2.70	3.10	3.10	0.0	0.56	0.030	0.030	0.060
V207S135C	Bal.	12.00	3.0	4.3	0.60	2.8	0.00	3.40	2.50	3.90	3.20	0.0	0.00	0.030	0.030	0.060
V207S135D	Bal.	11.30	3.0	4.3	0.60	3.4	0.56	3.30	2.40	3.90	3.20	0.0	0.00	0.030	0.030	0.060
V207S135E	Bal.	11.80	3.0	4.3	0.60	3.1	0.56	3.60	2.50	4.60	2.00	0.0	0.00	0.030	0.030	0.060
V207S135F	Bal.	11.40	2.0	5.3	0.60	3.2	0.57	3.50	2.50	3.90	2.80	0.0	0.00	0.030	0.030	0.060
V207S135G	Bal.	11.80	4.0	3.3	0.60	3.5	0.56	3.50	2.50	3.90	2.80	0.0	0.00	0.030	0.030	0.060
V207S135H	Bal.	12.20	4.0	3.3	0.58	3.1	0.56	3.60	2.50	4.60	2.00	0.0	0.00	0.030	0.025	0.055
V207S135I	Bal.	12.20	4.0	3.3	0.57	3.1	0.55	3.60	2.50	4.60	2.00	0.3	0.00	0.030	0.025	0.055
V207S135J	Bal.	12.30	4.0	3.4	0.58	3.2	0.55	3.60	2.70	4.70	1.60	0.0	0.00	0.050	0.025	0.055
V207S135K	Bal.	12.00	4.0	3.3	1.50	3.1	0.55	3.50	2.90	4.60	1.60	0.0	0.00	0.050	0.025	0.055

**[0012]** The inventors have also determined that alloys, which show combinations of Al, Ti, Nb, Ta and Si additions between 12.5 and 13.5 atomic % offer a further balance of properties in terms of environmental resistance and high temperature strength/ resistance to primary creep. Examples of such alloys are presented in Table 4.

**[0013]** A high volume fraction of small  $\gamma'$  precipitates will effectively hinder the movement of dislocations and will give rise to good high temperature proof strength. Ideally, secondary  $\gamma'$  particles of 50 to 300 nm in size should be developed after quenching the alloy from the solution heat treatment temperature. It is proposed that such particle sizes can be achieved in large diameter (500-700 mm) forgings using forced compressed/fan air cooling, particularly if attention is paid to the definition of compositions in which the temperature for secondary  $\gamma'$  precipitation is minimised. This assertion is based on the principle that rates of diffusion are less at lower temperature so that the driving force for particle coarsening is reduced. Similarly, alloy composition will determine the  $\gamma'$  solvus temperature, i.e. the temperature at which all  $\gamma'$  particles dissolve into solution. The amount of Al in the alloy has the most significant influence on the  $\gamma'$  solvus temperature, with higher quantities increasing the solvus temperature. However, reducing the amount of cobalt (Co), and Ti in the composition, a proportion of which partitions to the  $\gamma'$  phase, will reduce the  $\gamma'$  solvus temperature. Silicon is also known to reduce  $\gamma'$  solvus temperature. In two of the proposed compositions (V207S125E and V207S135B), the addition of about 1.15 at.% Si is expected to reduce the  $\gamma'$  solvus temperature of the Group 1 and 2 alloys by 7-16°C and 6-11°C respectively.

Table 3 - Predicted values of  $\gamma'$  %, phase solvus temperatures, density, % misfit and solid solution strength contribution ( $\Delta\sigma$ ) for proposed compositions and RR1000

Alloys	$\gamma'$ % at 800°C	$\gamma'$ solvus (°C)	$M_{23}C_6$ solvus (°C)	$\sigma$ solvus (°C)	density (g.cm <sup>-3</sup> )	% misfit at 800°C	$\Delta\sigma$ (MPa)
RR1000	43	1139	776	917	8.21	0.12	230
V207S125A	48	1109	860	659	8.34	0.38	187
V207S125B	48	1108	874	690	8.33	0.37	189
V207S125C	49	1115	893	648	8.30	0.33	187
V207S125D	48	1117	830	670	8.32	0.33	187
V207S125E	48	1101	859	665	8.28	0.26	187
V207S125F	48	1114	861	634	8.34	0.44	184
V207S125G	49	1113	878	646	8.36	0.32	192
V207S125H	49	1113	904	647	8.37	0.29	192
V207S125I	48	1106	885	643	8.37	0.31	190
V207S125J	49	1113	895	670	8.39	0.33	193
V207S125K	49	1111	898	663	8.40	0.34	190
V207S125L	49	1114	960	653	8.34	0.27	191
V207S125M	49	1122	985	637	8.46	0.22	211
V207S135A	53	1127	842	661	8.37	0.38	183
V207S135B	54	1121	838	670	8.29	0.25	182
V207S135C	53	1132	843	635	8.38	0.44	180
V207S135D	53	1129	822	613	8.43	0.36	186
V207S135E	53	1133	881	642	8.39	0.31	186
V207S135F	53	1129	843	605	8.36	0.34	182
V207S135G	54	1136	856	638	8.40	0.34	187
V207S135H	54	1147	909	674	8.38	0.28	186
V207S135I	54	1148	846	684	8.40	0.28	186
V207S135J	54	1135	911	652	8.36	0.30	186
V207S135K	55	1144	982	677	8.46	0.18	209

(continued)

Alloys	$\gamma'$ % at 800°C	$\gamma'$ solvus (°C)	$M_{23}C_6$ solvus (°C)	$\sigma$ solvus (°C)	density (g.cm <sup>-3</sup> )	% misfit at 800°C	$\Delta\sigma$ (MPa)
S1325A	53	1139	986	669	8.46	0.18	209
V211B	51	1134	921	684	8.45	0.27	202
V210B	51	1124	942	711	8.41	0.15	212

Table 4 - Examples of compositions in between Groups 1 and 2

at.%	Ni	Cr	Co	Fe	Mo	W	Mn	Al	Ti	Ta	Nb	C	B	Zr
S1325A	Bal	14.00	4.0	0.0	1.15	1.15	0.59	7.50	3.35	1.50	0.90	0.245	0.135	0.0355
V211B	Bal	14.25	8.3	0.0	1.00	1.10	0.59	7.25	3.25	1.50	0.90	0.245	0.135	0.0355
V210B	Bal	13.75	3.5	4.6	1.00	1.00	0.00	8.25	2.25	1.25	1.25	0.150	0.135	0.0355
wt.%	Ni	Cr	Co	Fe	Mo	W	Mn	Al	Ti	Ta	Nb	C	B	Zr
S1325A	Bal	12.40	4.0	0.0	1.90	3.60	0.55	3.45	2.75	4.60	1.40	0.050	0.025	0.055
V211B	Bal	12.60	8.3	0.0	1.60	3.45	0.55	3.35	2.65	4.60	1.40	0.050	0.025	0.055
V210B	Bal	12.30	3.5	4.4	2.00	3.80	0.00	3.80	1.80	3.90	2.00	0.030	0.025	0.055

**[0014]** Solution heat treatment above the  $\gamma'$  solvus temperature is necessary to produce the required grain size for optimising dwell crack growth resistance. If the  $\gamma'$  solvus is high and close to the solidus temperature of the alloy, incipient melting and grain boundary boron (B) liquation can occur during solution heat treatment, as can quench cracking of the forging from fast cooling, following solution heat treatment. Since the  $\gamma'$  solvus temperature determines whether the alloy is viable for high temperature discs, the alloy composition needs to be defined to minimise the  $\gamma'$  solvus temperature. Hence the need for careful selection of Al, Co and Ti levels.

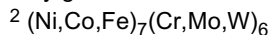
**[0015]** The contribution of Nb and Ta to  $\gamma'$  is important as these elements show slower rates of diffusion in Ni compared to Al and Ti, which is significant during quenching of forgings and high temperature operation in terms of reducing the rate of coarsening of secondary and tertiary  $\gamma'$  respectively, and in terms of resistance to oxidation damage since Al and Ti readily migrate from  $\gamma'$  to form oxidation products.

**[0016]** To optimise resistance to hot corrosion and oxidation, a protective chromia (Cr<sub>2</sub>O<sub>3</sub>) scale should form as quickly as possible at temperatures above 500°C. Three features of the proposed compositions facilitate this: firstly, to maximise the chromium (Cr) level in the  $\gamma$  phase; secondly, to minimise the Co and iron (Fe) content in the  $\gamma$  phase; and thirdly, to minimise the occurrence of rutile (TiO<sub>2</sub>) by reducing the Ti content. To promote the formation of a stable chromia scale, the inventors have determined that at temperatures between 500°C and 800°C, the Cr level in the  $\gamma$  should be greater than 25 at.%, and that the combined levels of Co and Fe be below 15 at.%. Figure 3 shows the predicted elemental content in the  $\gamma$  phase for alloy V207S135B.

In the alloys defined in Tables 1, 2 and 4, surface scales at temperatures between 650-800°C will be composed predominantly of Cr and Ti oxides, with initial transient oxides based on Cr, Ti and Ni, Fe and Co. The level of Cr that can be added is limited by the propensity for topological close packed (TCP) phases such as sigma ( $\sigma$ )<sup>1</sup>, mu ( $\mu$ )<sup>2</sup> and <sup>1</sup>(Ni, Co,Fe)<sub>x</sub>(Cr, Mo,W)<sub>y</sub> where x and y can vary between 1 and 7

**[0017]** P<sup>3</sup> during prolonged high temperature exposure. As an example, Table 3 shows  $\sigma$  solvus temperature for the proposed compositions. The solvus temperatures for the TCP phases were predicted from phase diagram modelling using JMat Pro v6.1 and the Thermatech Nickel-8 database. They are below or around 700°C, which indicates that on the basis of thermodynamics, these TCP phases are expected to form after a long exposure. In practice, TCP phases are considered unlikely to form at these low temperatures. They are much more likely to form if the solvus temperatures were at a higher temperature such as 800 or 900°C. The viability of the compositions in Tables 1, 2 and 4 were evaluated by predicting the  $\sigma$ ,  $\mu$  and P solvus temperature for the target chemistry plus the expected deviation that would be added to create a material specification, i.e. the TCP solvus temperatures were predicted for the upper limits of the elements in the material specification. These solvus temperatures should be below 800°C. This approach ensures that all possible variations in elemental content within the material specification will be free of TCP phases. It is important that alloys are free from these phases since they often precipitate at grain boundaries, reducing grain boundary strength and corrosion/oxidation resistance. They are therefore detrimental to material properties.

**[0018]** The proposed compositions show relatively high concentrations of Cr (12.5 to 15.5 at.%) for alloys with high volume fractions of  $\gamma'$ , the level of Cr being determined by the amount of  $\gamma'$ , molybdenum (Mo), tungsten (W), Fe and Co present. This is made possible in the higher Cr alloys by minimising the Mo content to about 0.35 at.% and the tungsten (W) content to about 1.1 at.%. Such low levels of Mo and W will increase coherency strains that arise because the  $\gamma'$  phase has a larger lattice parameter than the  $\gamma$  phase. To increase the Cr level beyond 16 at.% would require a further reduction of the  $\gamma'$ , Mo, W, Fe and Co content. However, greater differences in lattice parameter between  $\gamma$  and  $\gamma'$  phases may give rise to instabilities in the  $\gamma'$  phase, such as



$^3 \text{Cr}_{18}(\text{Mo,W})_{42}(\text{Ni,Co,Fe})_{40}$  discontinuous coarsening. These low values of Mo and W may also reduce the degree of substitutional solid solution strengthening<sup>4</sup> of the  $\gamma$  phase ( $\Delta\sigma$  in Table 3), which is necessary for producing the required high temperature strength and resistance to creep strain deformation. The amounts of Mo and W have been increased in alloys V207S125M, V207S135K, S1325A, V211A and V210B to raise the predicted solid solution strengthening<sup>4</sup> to levels that approach those predicted in existing high temperature Ni disc alloys such as RR1000, ME3 and LSHR. Whilst higher values of W and Mo are therefore appealing, the benefits from improved solid solution strengthening and reduced coherency strain need to be considered with the less appealing prospects of TCP formation, and the associated detriment to material properties, a reduced resistance to Type II hot corrosion as a result of acidic oxides and an increased alloy density. It is understood that much higher amounts of W and Mo than those specified in this invention are necessary for forming  $\text{M}_6\text{C}$  carbide from primary MC carbides. Such  $\text{M}_6\text{C}$  carbides are also detrimental to material properties.

**[0019]** Table 3 shows the predicted maximum misfit between the  $\gamma$  and  $\gamma'$  phases calculated at 800°C from predictions of lattice parameter for the  $\gamma$  ( $a_\gamma$ ) and  $\gamma'$  ( $a_{\gamma'}$ ) phases. Misfit or coherency strain ( $\delta$ ) is defined as:

$$\delta = \frac{a_{\gamma'} - a_\gamma}{a_\gamma} \quad (1)$$

**[0020]** The proposed compositions show greater predicted coherency strains than RR1000, which is expected to have a value of 0.12% at 800°C (Table 3). However, the predicted values in Table 3 are not considered to be excessive and should provide some additional strengthening through coherency strain, at least at low temperatures. It is also expected that deformation behaviour in the proposed alloys will be characterised by shearing of  $\gamma'$  particles by either anti-phase boundary coupled super lattice dislocations or by intrinsic/extrinsic stacking faults.

<sup>4</sup>H.A. Roth et al, (1997), Met. Trans., 28A (6), pp. 1329-1335.

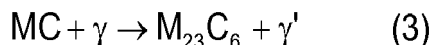
**[0021]** In the proposed compositions, the Co and Fe content in the  $\gamma$  phase has been minimised to enhance the effectiveness of Cr. In particular, the Co content has been reduced compared to those levels of Co (18.5-20.5 wt.%) in existing disc alloys such as RR1000, ME3, LSHR and Alloy 10, such that

$$\text{Fe} + \text{Co} < 8.5 \text{ at.}\% \quad (2)$$

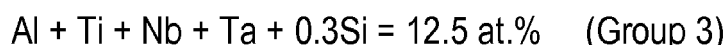
in which Fe can have values between about 0 and about 5.5 at.% and Co can have values between about 2.0 and about 8.5 at.%. The lower Co content also has benefits in reducing the propensity for  $\sigma$  phase precipitation and in reducing elemental costs. It is recognised, however, that Co in significant quantities (> 20 at.%) is beneficial in lowering stacking fault energy of the  $\gamma$  phase and in promoting annealing twins. This is important, particularly for solid solution strengthened alloys, since there is a direct correlation between creep rate and stacking fault energy. It is noted that other alloying additions such as Ti, Mo, W, manganese (Mn) and Cr also influence the number of stacking faults and the stacking fault energy in the  $\gamma$  phase and that precipitation strengthening, and the rate of diffusion of substitutional solute atoms (W, Mo in particular) in nickel also determine the resistance of nickel disc alloys to creep deformation.

**[0022]** Additional improvements can be made to the oxidation and hot corrosion resistance by further promoting chromia scale formation, by adding a sufficient quantity either of Si, to produce a silica ( $\text{SiO}_2$ ) film, and/or of Mn, to produce a spinel ( $\text{MnCr}_2\text{O}_4$ ) film beneath the chromia scale. It is predicted that Si and Mn partition between  $\gamma$  and  $\gamma'$  phases, residing predominantly in the  $\gamma$  phase above 500 °C. At such temperatures, nickel alloys begin to show signs of oxidation damage. Figure 4 shows the predicted partitioning of Si in the  $\gamma$  and  $\gamma'$  phases as a function of temperature for alloy V207S125E. Figure 5 (for alloy V207S125A) shows that the majority of Mn is present in the  $\gamma$  phase. It is also recognised that Si promotes the formation of  $\sigma$  phase, which requires that the Cr content in the alloy be reduced to maintain a stable microstructure. This potentially minimises any benefit from adding Si. Manganese, at levels of 0.2-0.6 wt.%, has been previously shown (US 4,569,824) to improve corrosion resistance at temperatures between 650-760°C and creep properties of polycrystalline nickel alloys, which contain 12-20 wt.% Cr.

**[0023]** Sufficient quantities of Nb, Ta and Hf are added to develop stable primary MC carbides (where M can represent Ti, Ta, Nb, or Hf) (Figure 6). Primary carbides based on Ti are not stable and, during prolonged exposure to temperatures above 700°C, decompose to  $M_{23}C_6$ , *i.e.*



**[0024]** These  $M_{23}C_6$  carbides form as films or elongated particles on grain boundaries and can reduce creep stress rupture life if extensive films decorate grain boundaries. It is understood that the formation of  $M_{23}C_6$  carbides removes Cr from the  $\gamma$  phase adjacent to the grain boundary, and therefore reduces the resistance to oxidation in this region. If thermal and fatigue loading conditions do not give rise to fatigue cracks, then Cr from near-surface  $M_{23}C_6$  carbides can diffuse along grain boundaries towards the surface, leaving voids. These voids are a form of internal oxidation damage, which can reduce the resistance of the alloy to fatigue crack nucleation. To optimise resistance to surface oxidation resistance, it is proposed that a further group of compositions be defined, *i.e.*



such that Al is about 7.0-7.5 at.%, Ti can have values between about 1.5 and about 2.0 at.%, Nb can have values between about 2.0 and about 2.5 at.%, Ta can have values between about 1.0 and about 1.5 at.% and Si can have values between zero and about 1.2 at.%. These alloys will show stable MC carbide and will be free of  $M_{23}C_6$  carbide.

**[0025]** It is proposed that the level of carbon (C) in the compositions is between about 0.1 and about 0.29 at.% (0.02 - 0.06 wt.%). A value of about 0.03 wt.% minimises internal oxidation damage from decomposition of  $M_{23}C_6$  carbides. However, this level of C is not as effective as 0.05 wt.% C in controlling grain growth through grain boundary pinning during super-solvus solution heat treatment. It is understood that the higher concentration of C produces a smaller average grain size and a narrow grain size distribution, with lower As Large As grain sizes. This is significant as yield stress and fatigue endurance at intermediate temperatures (< 650°C) are highly sensitive to grain size.

**[0026]** It has been found<sup>5,6</sup> that appropriate additions of zirconium, Zr, (in the region of 0.05-0.06 wt.%) and boron, B, (in the region of 0.02-0.03 wt.%) are required to optimise the resistance to intergranular crack growth from high temperature dwell fatigue cycles. In the development of both cast and forged polycrystalline superalloys for gas turbine applications, Zr is known to have improved high temperature tensile ductility and strength, creep life and rupture strength. Zirconium has an affinity for oxygen ( $O_2$ ) and sulphur (S) and scavenges these elements, thereby limiting the potential of  $O_2$  and S to reduce grain boundary cohesion. The role of B is less clear. It is understood that it is elemental B that improves grain boundary cohesion rather than the formation of grain boundary  $M_3B_2$  borides (where M = Mo or W). However, B can be detrimental if added in sufficient quantities as grain boundary films can form, particularly if high solution heat treatment temperatures are required.

**[0027]** It is also understood that limited precipitation of  $M_{23}C_6$  carbides and  $M_3B_2$  borides as particles on grain boundaries can be beneficial for dwell crack growth resistance. There should be sufficient particles on the grain boundaries to (1) minimise grain boundary sliding during dwell fatigue cycles and (2) to provide barriers to stress assisted diffusion of  $O_2$  along grain boundaries. In Tables 1, 2 and 4, the balance of Ti versus Nb, Ta and Hf in the proposed compositions has been defined to enable  $M_{23}C_6$  carbides to be precipitated at, or above, 820°C. This is shown in Table 3 by the

<sup>5</sup> C.J. Small, N. Saunders, (1999), MRS Bulletin, April 1999, pp. 22-26.

<sup>6</sup> E.S. Huron et al, (2004), Superalloys 2004, (Ed. K.A. Green et al), TMS (The Minerals, Metals & Materials Society), Warrendale, Pennsylvania, USA, pp. 73-81. predicted values of the  $M_{23}C_6$  carbide solvus temperature. The phase diagram modelling that was used in this invention suggests that Hf is the most potent MC stabilising element followed by Nb and Ta. However, very little of the Hf that is added to the alloy will be found in MC carbides. As with Zr, much of the added Hf scavenges available  $O_2$  and S. Where the levels of Hf exceed about 0.35 wt.%, there is sufficient Hf to partition to  $\gamma'$ , increasing the  $\gamma'$  solvus temperature and improving strength and resistance to creep strain accumulation. Whilst Hf is a very useful alloying addition, the affinity for  $O_2$  produces Hf oxide particles/inclusions during melting of the alloy. These melt anomalies need to be managed, and the occurrence of them balanced against the likely benefits for a particular alloy.

**[0028]** It is proposed that the size and location of MC carbides will influence the extent of the transformation shown in equation (3). The use of established powder metallurgy technology to produce alloy billet minimises the size of MC carbides in heat treated forgings to below 1  $\mu\text{m}$  in diameter. After solution heat treatment above the  $\gamma'$  solvus temperature, the majority (80-90%) of the MC carbides reside within grains rather than on grain boundaries. As diffusion is the driving force for the transformation, heat treatment temperature and time, and the distance that the MC carbide particle is to the nearest grain boundary will determine the extent of  $M_{23}C_6$  precipitation. A high temperature stabilisation heat treatment

at 830-870°C for 2 to 16 hours is required to precipitate limited amounts of  $M_{23}C_6$  carbide particles on grain boundaries. Furthermore, it is proposed that between 0.1 to 0.5 wt.%  $M_{23}C_6$  carbide is required to improve dwell crack growth behaviour.

**[0029]** The high temperature stabilisation heat treatment that is necessary for precipitating the required decoration of  $M_{23}C_6$  carbides on grain boundaries will also significantly coarsen tertiary  $\gamma'$  particles. Such coarsening will reduce the resistance of the alloy to primary creep and lower the high temperature yield stress. This is considered to be beneficial for material ahead of the crack tip in order to improve resistance to intergranular dwell crack growth, as it results in relaxation of crack tip stresses during the dwell period. However, finer tertiary  $\gamma'$  particles are required for good resistance to primary creep and high elevated temperature yield strength elsewhere in the alloy. These fine particles can be precipitated from a supplementary heat treatment, after the stabilisation heat treatment, at temperatures of between 800 and 850°C for 2 to 8 hours.

**[0030]** Work in the literature suggests that the effect of Nb on dwell crack growth behaviour of nickel disc alloys can vary significantly. Firstly<sup>8</sup>, evidence for cast and wrought alloys such 718 shows that Nb is detrimental to dwell crack growth as a result of the oxidation of large blocky MC carbides and delta ( $\delta$ ),  $Ni_3Nb$ , phase, which reside on grain boundaries and form brittle  $Nb_2O_5$ . It is also understood that a small fraction of the available Nb partitions to the  $\gamma$  phase and may segregate to grain boundaries in material ahead of a growing crack as a result of chromium<sup>9</sup> depletion from the  $\gamma$  phase as chromia forms from exposure to oxygen. Oxygen diffusion along grain boundaries is accelerated as a result of stress, particularly in material ahead of a crack tip during dwell fatigue cycles. The formation of  $Nb_2O_5$  is particularly detrimental as it produces a large volume change, as indicated by the Pilling-Bedworth Ratio of 2.5<sup>10</sup>, and readily cracks or spalls.

<sup>8</sup>M. Gao et al, (1994), Superalloys 718, 625, 706 and Various Derivatives, (Ed. By E.A. Loria), The Minerals, Metals & Materials Society, Warrendale, Pennsylvania, USA, pp. 581-592.

<sup>9</sup> A. Chyrkin et al, (2011), Oxid Met, 75, pp.143-166.

<sup>10</sup>J.P.S. Pringle, (1980), Electrochimica Acta, 25(11), pp. 1420-1437.

**[0031]** Work at NASA<sup>11</sup> on powder Ni disc alloy Alloy 10 indicates that the effect of Nb (up to about 1.7 wt.%) is less important than microstructural effects such as grain size and size of  $\gamma'$  particles. As the intention is to use powder metallurgy to produce the proposed compositions, Nb levels of up to about 2 at.% (or about 3.2 wt.%) have been added in the alloys in Tables 1, 2 and 4. Higher levels of up to about 2.5 at.% (or about 4 wt.%) Nb are proposed in the Group 3 alloys that contain lower concentrations of Ti and show no  $M_{23}C_6$  carbide. These alloys are optimised for oxidation resistance and not necessarily resistance to intergranular dwell crack growth. Results of phase diagram modelling using JMat Pro v6.1 and the Thermotech Nickel-8 database suggests that Nb does increasingly partition to  $\gamma$  at temperatures above 600°C. For Nb levels of 2 at.%, the predicted mole fraction of Nb in  $\gamma$  at 800°C is 0.3%. Whilst these concentrations are considered to be small, the Nb level in the alloy composition should be minimised to optimise dwell crack behaviour, as in V207S125L to values of about 0.75 at.% and in V207S125M, S1325A and V211 B to values of about 0.9 at.% respectively.

**[0032]** Titanium is beneficial to nickel alloys strengthened by  $\gamma'$  as it supplements Al in the ordered  $L1_2$  gamma prime particles and gives rise to high values of antiphase boundary (APB) energy when pairs of dislocations shear  $\gamma'$  particles. However, in addition to forming unstable MC carbides, Ti also gives rise to  $TiO_2$  (rutile) nodules that form above  $Cr_2O_3$  (chromia) nodules in the surface oxide scale. The source of Ti for the surface rutile nodules is considered to be  $\gamma'$ , and with the loss of Al from  $\gamma'$  for sub-surface alumina "fingers", a region free of  $\gamma'$  is produced during prolonged high temperature exposure. It is considered that this  $\gamma'$  free region shows significantly reduced proof strength compared to the base alloy and is likely to crack under conditions that lead to the accumulation of inelastic strain. To minimise these influences, Ti levels have been minimised in the proposed alloys, particularly the Group 3 compositions.

<sup>11</sup> J. Telesman et al, (2004), Superalloys 2004, (Ed. by K.A. Green et al), The Minerals, Metals & Materials Society, Warrendale, Pennsylvania, USA, pp. 215-224.

**[0033]** Levels of trace elements S and P should be minimised to promote good grain boundary strength and mechanical integrity of oxide scales. It is understood that levels of S and P of less than 5 and 20 ppm respectively are achievable in large production size batches of material. However, it is anticipated that the benefits of the invention would still be achievable provided the level of S is less than 20 ppm, and of P less than 60 ppm, although in these circumstances the resistance of the alloys to cracking from oxidation would be inferior.

**[0034]** It is envisaged that alloys according to the invention will be produced using powder metallurgy technology, such that small powder particles (<53  $\mu m$  in size) from inert gas atomisation are consolidated in a stainless steel container using hot isostatic pressing or hot compaction and then extruded or otherwise hot worked to produce fine grain size billet. Increments would be cut from these billets and forged under isothermal conditions. Appropriate forging temperatures, strains and strain rates would be used to achieve the preferred average grain size of ASTM 8 to 6 (22-45  $\mu m$ ) following solution heat treatment above the  $\gamma'$  solvus temperature.

**[0035]** To generate the required balance of properties in the alloys according to the invention, it is also necessary to

undertake the following heat treatment steps:

1. The preferred route is to solution heat treat the forging above the  $\gamma'$  solvus temperature to grow the grain size to the required average grain size of ASTM 8 to 6 (22-45  $\mu\text{m}$ ) throughout. Appropriate forging conditions, levels of deformation and heating rates in solution heat treatment will be used to achieve the required average grain size and prevent isolated grains from growing to sizes greater than ASTM 2 (180  $\mu\text{m}$ ).
2. Quench the forging from the solution heat treatment temperature to room temperature using forced or fan air cooling. The resistance to dwell crack growth is optimised if the cooling rate from solution heat treatment is defined so as to produce grain boundary serrations around secondary  $\gamma'$  particles<sup>12</sup>. Such serrations extend the distance for oxygen diffusion and improve the resistance to grain boundary sliding.
3. Undertake a stabilisation/stress relief and a subsequent precipitation heat treatment at temperatures between 800°C and 870°C for 2-16 hours, then air cool. These heat treatments are required to i) precipitate a limited decoration of  $\text{M}_{23}\text{C}_6$  carbide particles on grain boundaries; ii) relieve residual stresses from quenching; iii) precipitate a distribution of coarse and fine tertiary  $\gamma'$  particles.
4. If higher levels of yield stress and low cycle fatigue performance are required in the bore and diaphragm regions of the disc rotor at temperatures below 650°C, then a dual microstructure solution heat treatment (US 8,083,872) can be applied to forgings to produce a fine (5-10  $\mu\text{m}$ ) average grain size in these regions.

**[0036]** The proposed alloys are expected to show the following material properties compared to the existing nickel alloy RR1000, with the same grain size, and taking account of differences in density (8.21  $\text{g}\cdot\text{cm}^{-3}$  for RR1000; 8.28 - 8.5  $\text{g}\cdot\text{cm}^{-3}$  for the proposed compositions at ambient temperature).

**[0037]** Improved resistance to oxidation and hot corrosion damage at temperatures of 600-800°C; improved tensile proof strength at temperatures of 20-800°C; improved resistance to creep strain accumulation at temperatures of 650-800°C; dwell crack growth resistance equivalent or better than RR1000 at temperatures above 600°C; improved dwell fatigue endurance behaviour at temperatures above 600°C; similar or improved fatigue endurance behaviour to RR1000 at temperatures below 600°C; improved microstructural stability during high temperature exposure at 800°C or from stabilisation/precipitation heat treatment).

<sup>12</sup> R.J. Mitchell et al, (2009), J. Mater. Process. Tech., 209, pp. 1011-1017.

**[0038]** It is expected that the time to develop a life-limiting depth of hot corrosion and oxidation damage for Group 1 alloys will be twice that of existing alloys such as 720Li and RR1000 at temperatures between 650°C and 800°C.

**[0039]** The invention therefore provides a range of nickel base alloys particularly suitable to produce forgings for disc rotor applications. Components manufactured from these alloys will have a balance of material properties that will allow them to be used at significantly higher temperatures. In contrast to known alloys, the alloys according to the invention achieve a better balance between resistance to environmental degradation and high temperature mechanical properties such as proof strength, resistance to creep strain accumulation, dwell fatigue and damage tolerance. This permits the alloys according to the invention to be used for components operating at temperatures up to 800°C, in contrast to known alloys which are limited to temperatures of 700 - 750°C.

**[0040]** These improved properties are achieved by i) definition of compositions; ii) the process routes for billet and forgings; and iii) the heat treatment of the forgings. Particular attention has been given to i) producing 48-55 %  $\gamma'$  at 800°C; ii) minimising Al, Co and Ti content to reduce the  $\gamma'$  solvus temperature, which is likely to be high from such volume fractions of  $\gamma'$ ; iii) producing grain boundary morphology and phases to optimise resistance to intergranular dwell crack growth; iv) maximising Cr content, whilst minimising Co and Fe content in the  $\gamma$  phase to promote the formation of chromia scale as quickly as possible during exposure to high temperatures but without rendering the compositions prone to precipitation of detrimental grain boundary  $\sigma$  phase; v) minimising elements that are considered detrimental to oxidation and hot corrosion resistance; and vi) the addition of Mn and Si to promote stable  $\text{Cr}_2\text{O}_3$  scales through the formation of  $\text{MnCr}_2\text{O}_4$  and  $\text{SiO}_2$  and films.

**[0041]** Although the alloys according to the invention are particularly suitable for disc rotor applications in gas turbine engines, it will be appreciated that they may also be used in other applications. Within the field of gas turbines, for example, it is envisaged that they would be especially suitable for use in combustor or turbine casings, which would benefit from the expected improvements in material properties, notably the improved proof strength and resistance to creep strain accumulation. As compressor discharge temperatures and turbine entry temperatures increase over time, to promote improvements in thermal efficiency and thereby in fuel consumption, the temperature of the static components of the combustor and turbine will necessarily also increase. Such components could be produced by powder metallurgy given the highly alloyed compositions and the ability to produce compacts that are close to the component geometry, thereby reducing the amount of material required and the time required to machine the component.

## Claims

1. A nickel- base alloy having the following composition (in weight percent unless otherwise stated): Cr 10.5-15.0; Co 1.7-8.8; Fe 0-5.9; Si 0-0.65; Mn 0-0.65; Mo 0.3-2.3; W 2.3-4.4; Al 2.7-4.1; Nb 1.0-4.2; Ti 1.0-3.0; Ta 2.0-5.0; Hf 0.0-0.6; C 0.02-0.06; B 0.015-0.035; Zr 0.035-0.11; S < 20ppm; P < 60ppm; the balance being Ni and incidental impurities.
2. A nickel-base alloy having the following composition (in atomic percent unless otherwise stated): Cr 11.7-16.9; Co 1.7-8.75; Fe 0-6.2; Si 0-1.36; Mn 0-0.7; Mo 0.2-1.4; W 0.7-1.4; Al 5.8-8.8; Nb 0.63-2.65; Ti 1.2-3.7; Ta 0.6-1.6; Hf 0-0.2; C 0.1-0.29; B 0.08-0.19; Zr 0.022-0.071; S < 20ppm; P < 60ppm; the balance being Ni and incidental impurities.
3. The alloy of claim 2, having the following composition (in atomic percent): Al 6.5-8.25; Ti 2.25-3.5; Nb 0.75-2.25; Ta 0.75-1.5; Si 0-1.2; and in which the sum of the atomic percentages of Al, Ti, Nb and Ta and 0.3 of the atomic percentage of Si is between 12.5 at.% and 13.5 at.%.
4. The alloy of claim 3, in which the sum of the atomic percentages of Al, Ti, Nb and Ta and 0.3 of the atomic percentage of Si is 12.5 at.%.
5. The alloy of claim 3, in which the sum of the atomic percentages of Al, Ti, Nb and Ta and 0.3 of the atomic percentage of Si is 13.5 at.%.
6. The alloy of claim 2, having the following composition (in atomic percent): Al 7.0-7.5; Ti 1.5-2.0; Nb 2.0-2.5; Ta 1.0-1.5; Si 0-1.2; and in which the sum of the atomic percentages of Al, Ti, Nb and Ta and 0.3 of the atomic percentage of Si is 12.5 at.%.
7. The alloy of any one of claims 2 to 6, having the following composition (in atomic percent): Fe 0-5.5; Co 2.0-8.5; and in which the sum of the atomic percentages of Fe and Co is less than 8.5 at.%.
8. The alloy of any one of claims 2 to 7, having the following composition: S < 5ppm.
9. The alloy of any one of claims 2 to 8, having the following composition: P < 20ppm.
10. A method of making a nickel-base alloy, the method comprising the steps of:
  - a) producing a forging by a powder metallurgy technique, using powder having the composition of any one of the preceding claims;
  - b) solution heat treating the forging above the  $\gamma'$  solvus temperature so as to grow the average grain size to ASTM 8 to 6 (22 to 45  $\mu\text{m}$ ) throughout, while preventing individual grains from growing to sizes greater than ASTM 2 (180  $\mu\text{m}$ );
  - c) quenching the forging from the solution heat treatment temperature to room temperature by forced cooling or fan air cooling;
  - d) performing stabilisation/stress relief and precipitation heat treatments at a temperature between 800°C and 870°C for between 2 and 16 hours.
11. The method of claim 10, in which step a) comprises the steps of:
  - aa) consolidating small (<53  $\mu\text{m}$ ) powder particles from inert gas atomisation in a stainless steel container using hot isostatic pressing or hot compaction;
  - ab) using a hot working process to produce a fine grain size billet;
  - ac) cutting an increment from the billet and forging it under isothermal conditions.
12. The method of claim 10 or claim 11, in which in step c) the cooling rate is defined so as to produce grain boundary serrations around secondary  $\gamma'$  particles.
13. The method of any one of claims 10 to 12, in which the forging is in the form of a disc for a gas turbine engine, and further comprising the step of:
  - e) performing a dual microstructure heat treatment on the forging to produce a fine (5 to 10  $\mu\text{m}$ ) average grain

## EP 2 805 784 A1

size in a bore and a diaphragm region of the disc.

5

10

15

20

25

30

35

40

45

50

55

Figure 1

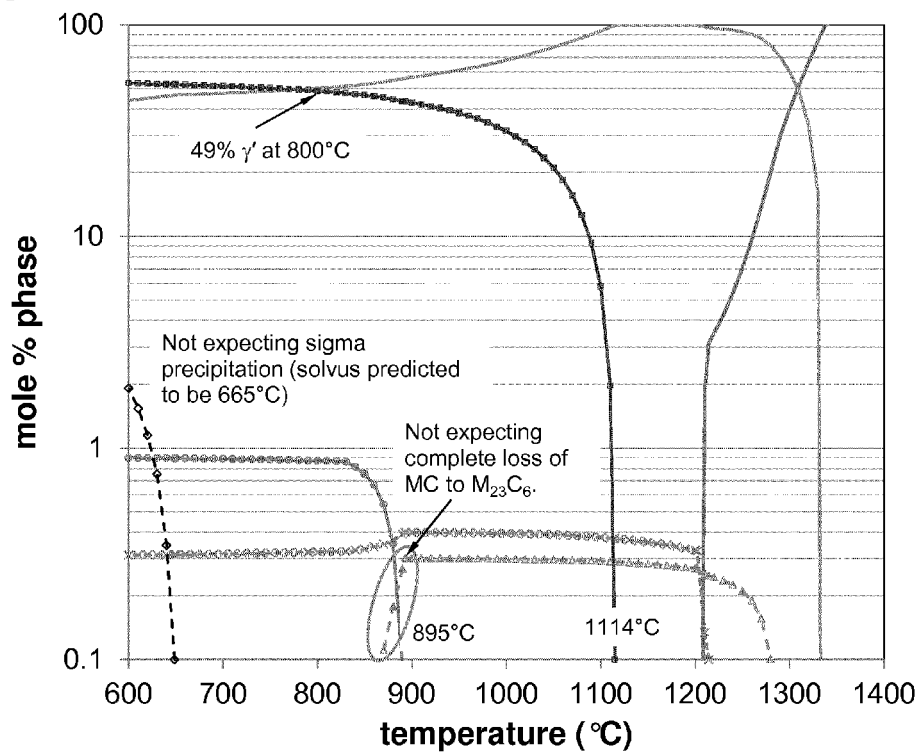


Figure 2

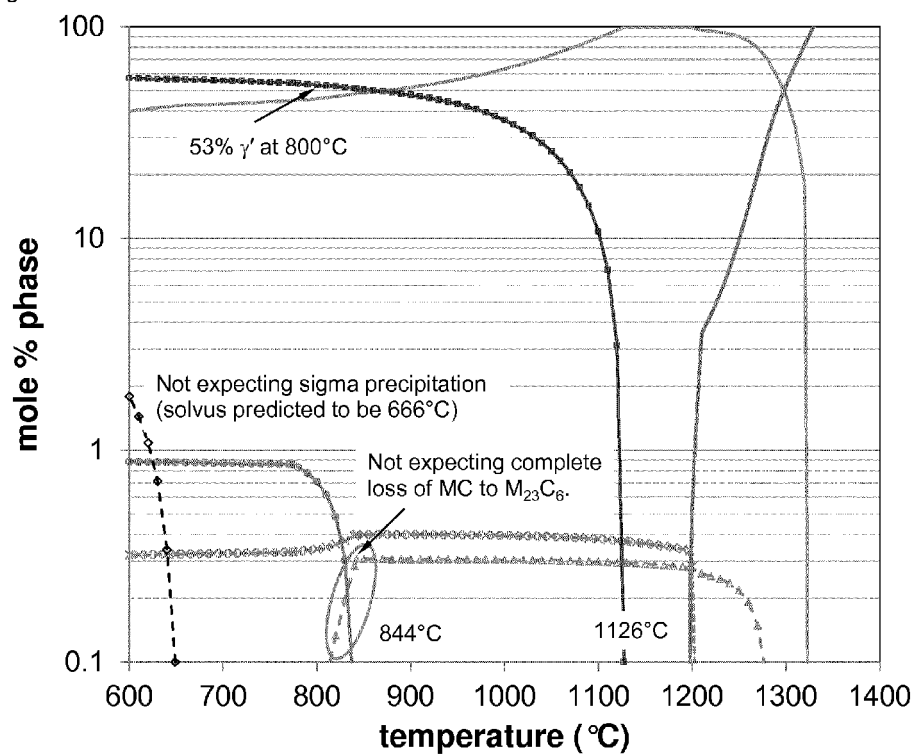


Figure 3

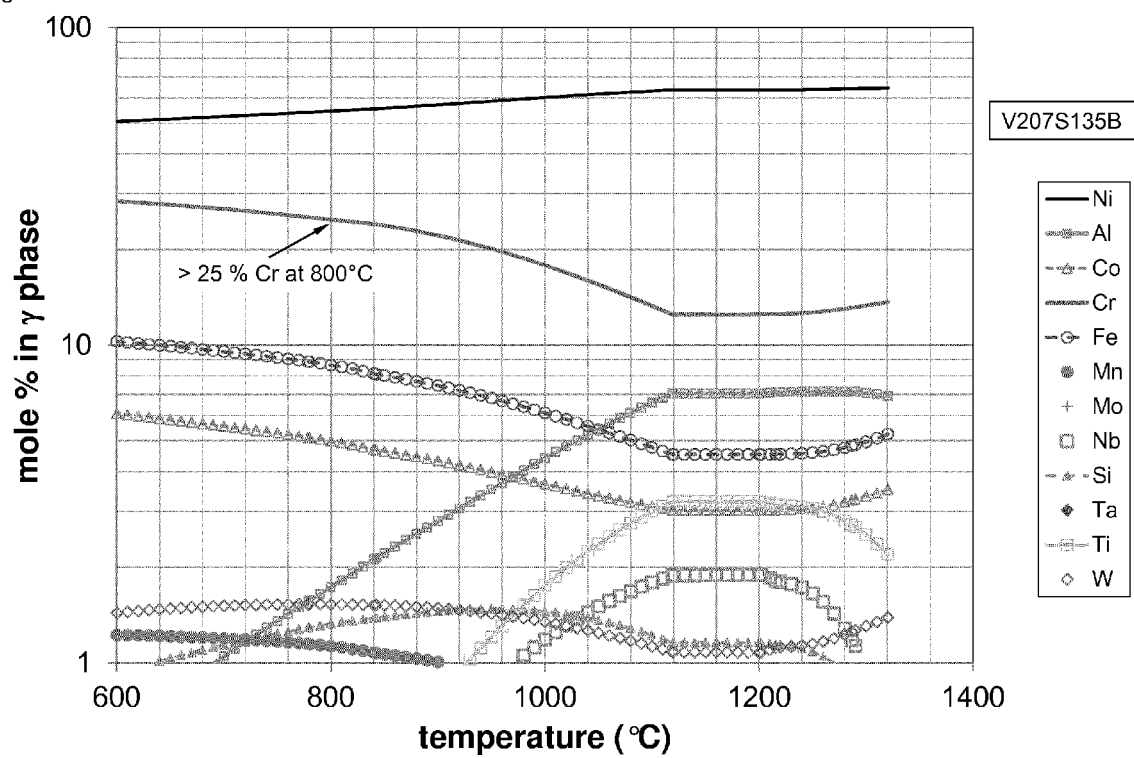


Figure 4

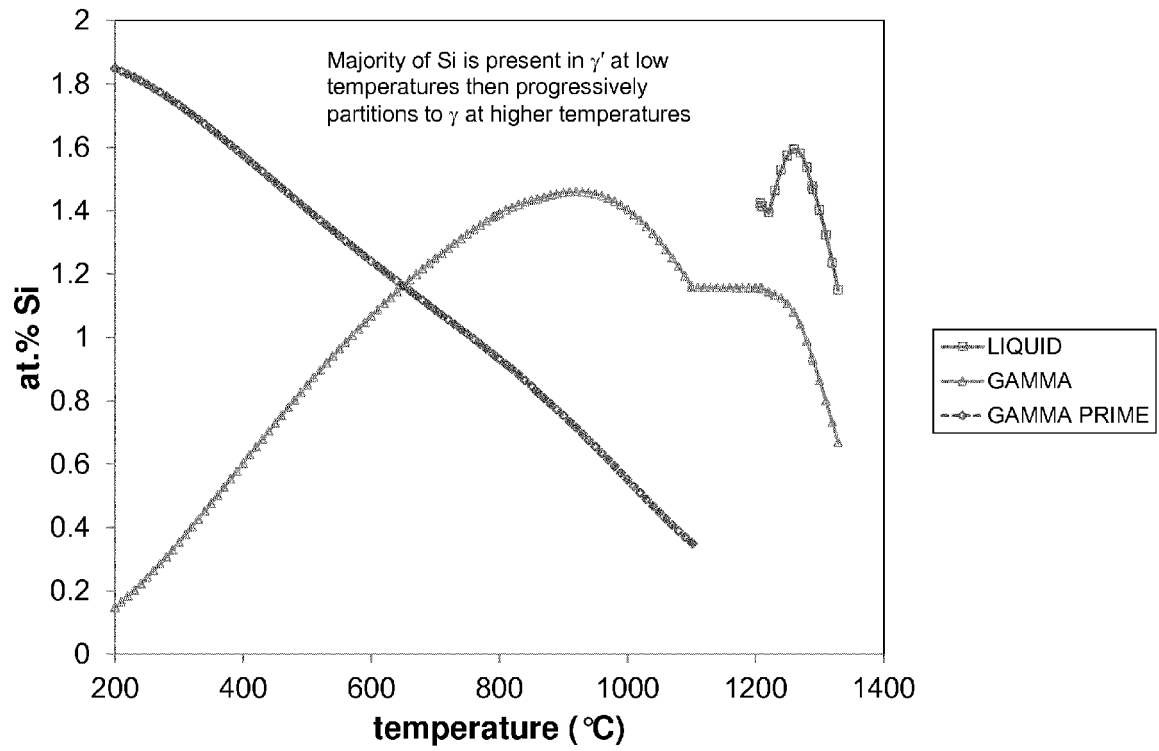


Figure 5

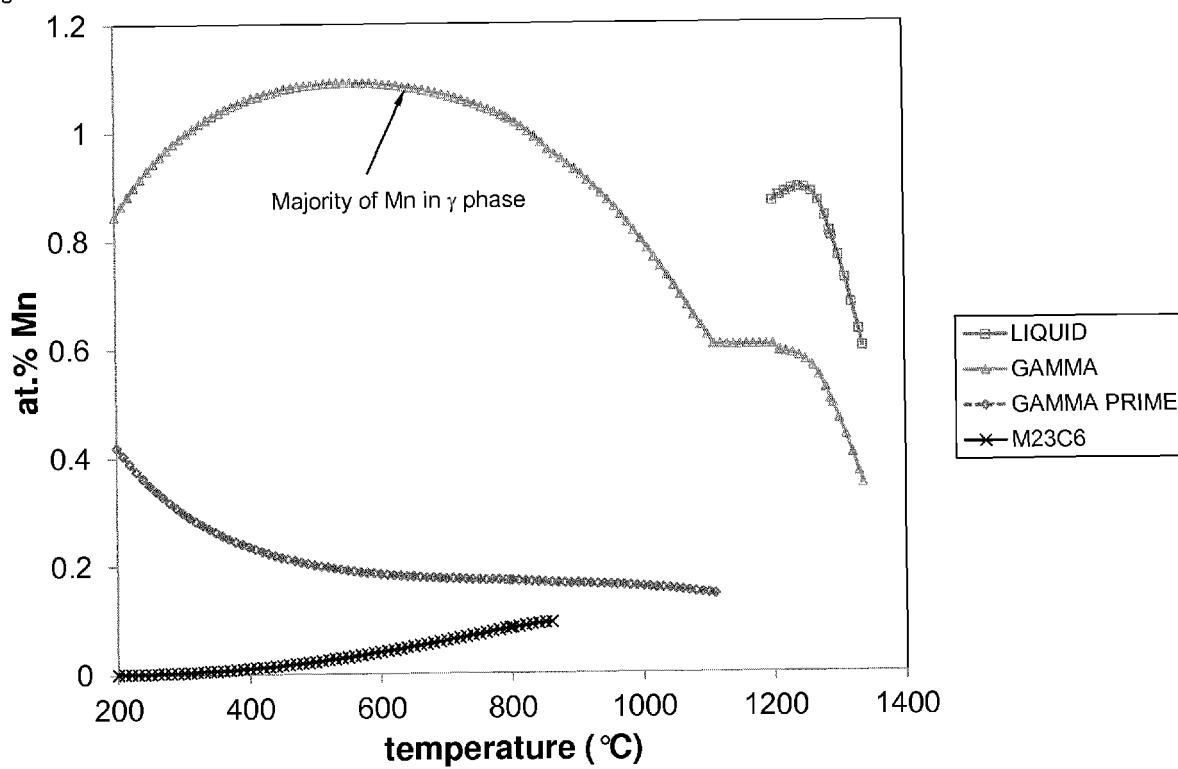
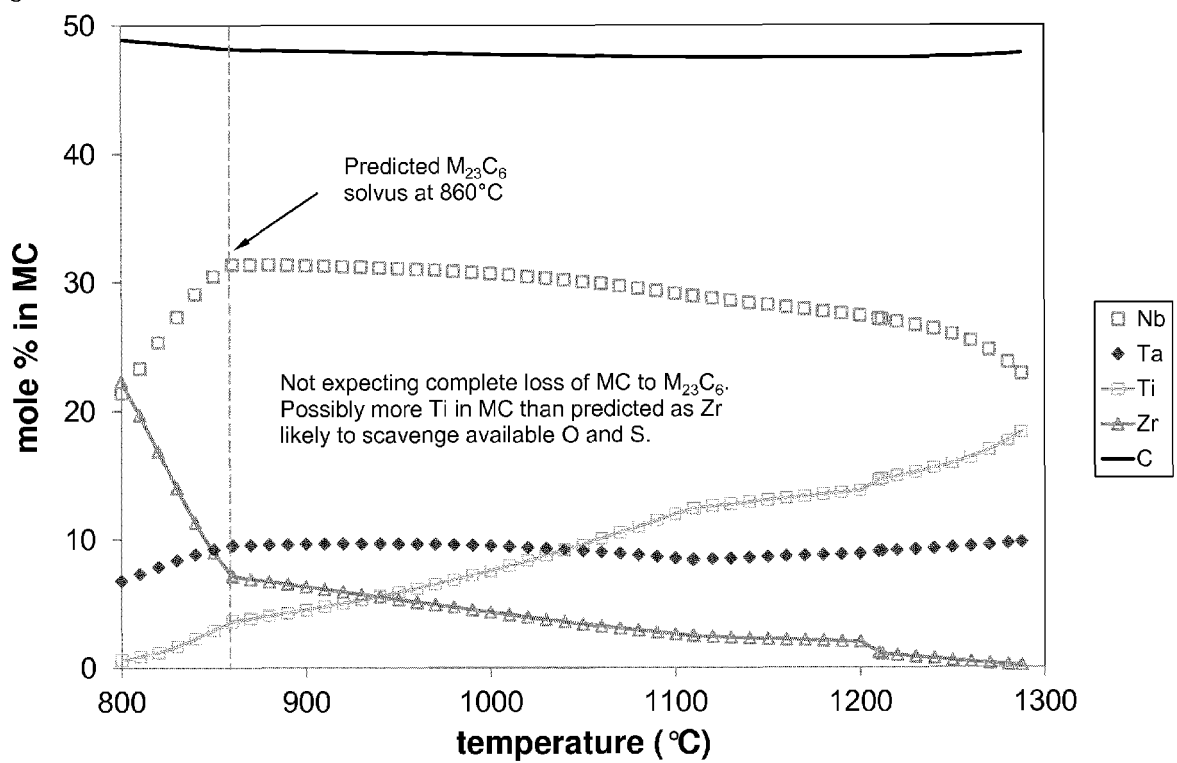


Figure 6





## EUROPEAN SEARCH REPORT

 Application Number  
 EP 14 15 7622

DOCUMENTS CONSIDERED TO BE RELEVANT			
Category	Citation of document with indication, where appropriate, of relevant passages	Relevant to claim	CLASSIFICATION OF THE APPLICATION (IPC)
A	CA 1 242 596 A1 (GEN ELECTRIC) 4 October 1988 (1988-10-04) * table 2(i)(ii) *	1-13	INV. B22F5/04 C22C19/05
A	EP 2 520 678 A2 (GEN ELECTRIC [US]) 7 November 2012 (2012-11-07) * tables 1-3 *	1-13	
A	EP 1 433 865 A1 (HITACHI LTD [JP]) 30 June 2004 (2004-06-30) * tables 1,2 *	1-13	
A	EP 0 561 179 A2 (WESTINGHOUSE ELECTRIC CORP [US] WESTINGHOUSE ELECTRIC CORP [CH]) 22 September 1993 (1993-09-22) * table 1 *	1-13	
A	EP 0 520 464 A1 (MITSUBISHI MATERIALS CORP [JP]; MITSUBISHI HEAVY IND LTD [JP]) 30 December 1992 (1992-12-30) * claims 1-8; tables 1-3 *	1-13	
			TECHNICAL FIELDS SEARCHED (IPC)
			C22C B22F
The present search report has been drawn up for all claims			
Place of search		Date of completion of the search	Examiner
Munich		16 May 2014	Badcock, Gordon
CATEGORY OF CITED DOCUMENTS X : particularly relevant if taken alone Y : particularly relevant if combined with another document of the same category A : technological background O : non-written disclosure P : intermediate document T : theory or principle underlying the invention E : earlier patent document, but published on, or after the filing date D : document cited in the application L : document cited for other reasons & : member of the same patent family, corresponding document			

EPO FORM 1503 03.82 (P04C01)

**ANNEX TO THE EUROPEAN SEARCH REPORT  
ON EUROPEAN PATENT APPLICATION NO.**

EP 14 15 7622

16-05-2014

This annex lists the patent family members relating to the patent documents cited in the above-mentioned European search report.  
The members are as contained in the European Patent Office EDP file on  
The European Patent Office is in no way liable for these particulars which are merely given for the purpose of information.

Patent document cited in search report	Publication date	Patent family member(s)	Publication date
CA 1242596	A1	04-10-1988	NONE
EP 2520678	A2	07-11-2012	CN 102766787 A 07-11-2012 EP 2520678 A2 07-11-2012 US 2012282086 A1 08-11-2012
EP 1433865	A1	30-06-2004	DE 60303971 T2 16-11-2006 EP 1433865 A1 30-06-2004 JP 4036091 B2 23-01-2008 JP 2004197131 A 15-07-2004 US 2004177901 A1 16-09-2004
EP 0561179	A2	22-09-1993	AU 3380093 A 23-09-1993 CA 2091827 A1 19-09-1993 CN 1076508 A 22-09-1993 EP 0561179 A2 22-09-1993 JP H0617171 A 25-01-1994
EP 0520464	A1	30-12-1992	CA 2072446 A1 28-12-1992 DE 69208538 D1 04-04-1996 DE 69208538 T2 11-07-1996 EP 0520464 A1 30-12-1992 US 5431750 A 11-07-1995 US 5516381 A 14-05-1996

EPO FORM P0459

For more details about this annex : see Official Journal of the European Patent Office, No. 12/82

## REFERENCES CITED IN THE DESCRIPTION

*This list of references cited by the applicant is for the reader's convenience only. It does not form part of the European patent document. Even though great care has been taken in compiling the references, errors or omissions cannot be excluded and the EPO disclaims all liability in this regard.*

### Patent documents cited in the description

- US 4569824 A [0022]
- US 8083872 B [0035]

### Non-patent literature cited in the description

- **H.A. ROTH et al.** *Met. Trans.*, 1997, vol. 28A (6), 1329-1335 [0020]
- **C.J. SMALL ; N. SAUNDERS.** *MRS Bulletin*, 1999, 22-26 [0027]
- **E.S. HURON et al.** *Superalloys. The Minerals, Metals & Materials Society*, 2004, 73-81 [0027]
- **H.-J. JOU et al.** *Superalloys. The Minerals, Metals & Materials Society*, 2012, 893-902 [0029]
- **M. GAO et al.** *Superalloys 718, 625, 706 and Various Derivatives. The Minerals, Metals & Materials Society*, 1994, 581-592 [0030]
- **A. CHYRKIN et al.** *Oxid Met*, 2011, vol. 75, 143-166 [0030]
- **J.P.S. PRINGLE.** *Electrochimica Acta*, 1980, vol. 25 (11), 1420-1437 [0030]
- **J. TELESMA et al.** *Superalloys 2004. The Minerals, Metals & Materials Society*, 2004, 215-224 [0032]
- **R.J. MITCHELL et al.** *J. Mater. Process. Tech.*, 2009, vol. 209, 1011-1017 [0037]